ORIGINAL PAPER

CrossMark

Numerical simulation of 2D granular flow entrainment using DEM

Chao Kang[1] · Dave Chan[1,2]

Abstract
To understand the entrainment process in granular flow, numerical experiments have been conducted using a Discrete Element Method model. A flow channel of 8 m long with 15° slope is setup with monitoring points located in an erodible bed. Particles, ranging from 3 to 4 mm in diameters, are used in the simulations. In the simulations, translational, rotational and average velocities, total volume, shear stresses are calculated in the measurement circles. The sizes of the measurement circles have been varied to see their effects on the results. It is found the minimum size of the measurement circles should include 20–30 particles. An new analytical model has been developed to calculate entrainment in granular flow. Results of the numerical experiment are compared with analytical model. Shear stresses at the interface between flowing particles in motion and the immobile particles in the channel bed, change of depth of erosion and entrainment rate are used to verify the analytical model. It is found that the calculated shear stresses in the PFC model agree well with the shear stresses calculated using Mohr–Coulomb frictional relationship in the analytical model. The calculated depth of erosion using the new analytical model is also compared with that from dynamic and static entrainment model. The results indicates that the analytical model is able to capture the mechanism of erosion and it can be used in granular flow analysis.

Keywords Granular flow · Entrainment · Numerical experiment · Debris flow · Discrete element method

1 Introduction

Debris flows can be defined as mass movement down a well defined channel, predominantly consisting of mixture of coarse granular material and mud that may contain large unsorted materials such as boulders, trees, and other debris (Hungr et al. 2014). It is usually fast-moving with variable solid concentration and large runout distance. Although many debris flows are saturated with water, there are some debris flows with little or no water in them, such as the dry debris flow which occurred at Nanarnawari, Mitaka-iriya, on the Izu Peninsula triggered by 1978 Izu-Oshima-Kinkai earthquake [8]. The mobility of debris flow is enhanced by the presence of water and sometimes fluidization of the material. Fluidization refers to the loss of shearing resistance of loose granular material under rapid shearing. Although it is often considered that the presence of water is required for

fluidization to occur, Melosh [37] concluded that air or water is not always necessary in some cases. Hungr and Evans [17] also found debris flow with no water in some cases.

When debris flows along a channel with loose deposit on the side or bottom of the channel, the debris will erode the channel material resulting in a substantially larger final volume than its initial volume [23,43,49]. This is called entrainment. Entrainment can significantly change the mechanics and characteristics of debris flow thus making prediction and back analysis of debris flow much more difficult [35]. There are many cases of debris flow with significant entrainment, such as Yigong rock avalanche (2000) in Tibet China, Eagle Pass Slide (1999) and Nomash River rockslide (1999) in British Columbia Canada [17,25]. Moreover, all of these cases have negligible water in the debris.

In order to calculate entrainment for debris flow, an analytical entrainment model has been developed which considers various mechanism of erosion and entrainment, such as rolling motion and shearing failure of the granular material. It is difficult to perform physical experiments or field observations that provide detail examination of the flow and entrainment processes. Therefore, a numerical approach using the discrete element method (DEM) is adopted to

✉ Chao Kang
  ckang3@ualberta.ca

1 Department of Civil and Environmental Engineering, University of Alberta, Edmonton, Canada

2 College of Civil Engineering and Architecture, Three Gorges University, Yichang, China

simulate granular flow and to understand the erosion and entrainment processes. In the numerical simulations, a flume with erodible bed is provided to examine the erosion of particles when a group for granular particles is released from higher elevation and passes thru the erodible zone. The entrained volume, displacement and average velocity of the granular flow are calculated. Rotational and transla-tional motions of the particles are also calculated and tracked at three locations in the erodible zone. Entrainment is exam-ined by calculating the motion of the particles when they reach sufficiently high velocity that it can be included in the flowing mass. Two mechanism have been examined; shear-ing failure in the erodible bed and rolling motions at the surface of the erodible bed. The time for the beginning of entrainment is compared with the time when shear failure occurs or when rolling motion begins. This will identify the mechanism of erosion. The entrainment model is evaluated by comparing the model calculation with the results from the DEM simulation. The depth of erosion from the analytical model is also compared with that calculated from the static and dynamic entrainment models proposed by Medina et al. [36].

2 Debris flow entrainment

2.1 Entrainment process

When rapid moving debris travels along channels covered by surficial deposits, sometimes several meters in thickness, it can cause erosion and increase the mass of the debris by inclusion [23]. The erosion process together with inclusion process is called entrainment. To understand entrainment in debris flow, experiments have been conducted using inclined flumes which have different sizes of tank, and different length of erosional zone and deposition pad ([13,31]; Iverson and Ouyang 2015). McCoy et al. (2010) and Berger et al. (2011) also carried out field tests and monitored the entrainment at specific locations. McCoy et al (2013) used an erosion sensor to measure changes in the height of the bed sediment after Berger et al. (2011). Moreover, incision bolts have been used to measure the average incision rate by McCoy et al. (2013).

2.2 Calculation of entrainment

There are several models in calculating the amount and rate of entrainment in debris flow analysis. The models can basically be classified into two approaches: the static approach and the dynamic approach. In the static approach, static shear stresses are calculated beneath the debris and failure is considered when the static shear stress exceeds the shear strength of the material. The depth in which failure occurs is determined and the amount of material is calculated which will be added to

the main body of the debris. In the dynamic approach, the rate of erosion is determined based on shear failure at the surface and the material is removed from the surface based on the velocity of flow of the main body of the debris [36].

Egashira et al. [13] proposed a formula to calculate the rate of erosion assuming that the slope of the channel bed is always adjusted to the angle corresponding to limiting equi-librium conditions. The material in the channel left behind by an unsaturated debris will approach the limiting equilibrium slope angle. Geometrical relationship between the initial bed slope and equilibrium slope angle is incorporated into the mass conservation law of the eroded material to obtain the entrainment rate.

The entrainment model proposed by van Asch et al. in 2004 [30] is a dynamic one dimensional debris flow model that takes into account the entrainment concept based on the generation of the excess pore water pressure under undrained loading on the in-situ material. Due to the moving mass flow-ing on top of the erodible bed, a loading on the bed deposits is generated. The model calculates this applied load on the in-situ soil through changes in the vertical normal stress and shear strength caused by the debris flow. The increase in pore water pressure is calculated based on the Skempton's [47] equation. The depth of erosion is approximated using the relationship between the factor of safety at the bottom and top of soil in the channel.

Iverson [23] considered the behavior of a slide block descending an erodible slope with the ability of incorporating soil on the static bed. Newton's second law was applied on the sliding material. Then, Coulomb friction rule was applied and basal friction resistance calculation was improved by taking the shear rate into account. The friction resistance consists of a constant component of friction resistance and a velocity-dependent component. After considering the rate-dependent friction, entrainment rate based on the change in weight of the sliding block was obtained. Iverson and Ouyang (2015) updated the equation for estimating basal erosion rate. Jump conditions at the interfaces between each layer, which descripts the sudden change of shear stress and horizontal velocity in the debris, were considered in the derivation.

2.3 Estimation of entrainment rate

Although several methods exist in the calculation of entrain-ment rate, when encountering dry granular flows, the calcu-lated results does not agree with the observations. Iverson [22] carried out a flume test on a slope, 31° with respect to horizontal, using a mixture of sand-gravel-mud (37% sand, 56% gravel, and 7% mud size (silt/clay) grains by dry weight). The erodible bed formed between 6 and 53 m downs-lope of the headgate, was consisted of the same material as that in the tank used to simulate granular flow. In the test, the mixture was released from the tank and 1–2 cm erosion

of material was observed showing an entrainment rate of 0.0032–0.0064 m/s on average.

Since static and dynamic entrainment models are mainly used in entrainment calculation, they are adopted here to estimate the rate or erosion. Reid et al. (2011) and Iverson et al. [22] monitored the normal pressure, pore water pressure and flow height in the experiment. The authors calculate the entrainment depth and erosion rates using static, dynamic and progressive scouring entrainment models, at the time when normal stress has maximum value. In the calculation, all the parameters were from published information (Reid et al. 2011; [22]). Moreover, two more calculations were also carried out 0.2 s before and after the appearance of maximum normal stress. They were named as t_1, t_2 and t_3 in chronological order. The calculated entrainment rates from static and dynamic models were smaller than zero at t_2 and t_3. The entrainment rate was approximately 0.0027 m/s at t_1. When progressive scouring model was used in the calculation, the rate of erosion at t_1, t_2 and t_3 were 0.0039, 0.0036 and 0.0037 m/s. The calculation results from the static and dynamic models at t_2 and t_3 indicated negative entrainment rates and the entrainment rate at t_1 was smaller than the average rate. In comparison, the rates calculated using progressive scouring model were always in the range of the average entrainment rate. Therefore, it is possible that there is another mechanism existing in the dry granular flow entrainment process.

2.4 A new entrainment model

It has been demonstrated that sediment entrainment will occur progressively from the sediment surface rather than by a mass failure along the bedrock-sediment interface (McCoy et al. 2012; Reid et al. 2011). In this study, an erosional mechanism that considers material lying on the channel bed being eroded progressively downward in a rolling motion is examined. This process is called progressive scouring. The current methods in entrainment calculations mainly consider shear failure under the channel bed. The equations to calculate the depth of entrainment based on basal shearing mode of erosion have been developed ([36]; Iverson and Ouyang 2015; Bouchut et al. 2016). However, the progressive scouring process in particle scale is also not considered in the models. This could lead to an error in estimating the rate of entrainment in granular flow.

In the new entrainment model, it is considered that granular particles lying on channel bed are eroded progressively [26]. Granular particles are abstracted as uniform size sphere (disk in the case of analysis). According to analysis carried out by Wu and Chou [48], Cheng et al. [7] and Shodja et al. [46], drag force to initiate rolling action is normally less than that required for basal shear failure. Therefore it is considered that rolling motion is the dominant motion in initial stage of
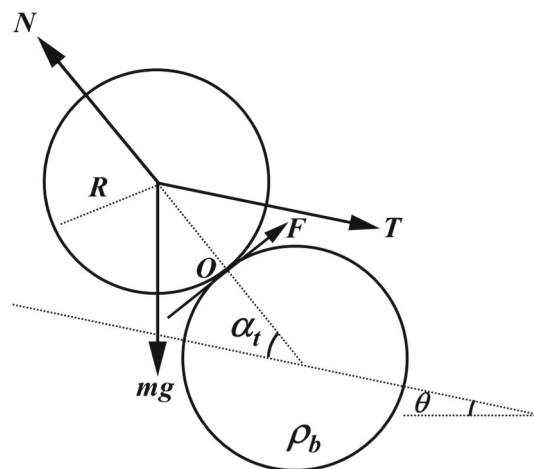

Fig. 1 Free body diagram of particle when rolling occurs

entrainment for granular material. However both rolling and shearing motions should be considered in the calculation of entrainment rate.

In calculating the drag force for the initiation of the rolling action, it is assumed that a particle will rotate around point O as shown in Fig. 1. Drag forces arising from the moving debris above the bed are assumed to apply at the center of the particle. It is assumed that the particle will rotate around the contact point with the adjacent particle located downstream. Newton's Law of Motion is applied to calculate the acceleration, velocity, and displacement of the particle. The equation governing the motion can be written as:

$$\frac{TR}{(I+mR^2)}\sin\alpha_t - \frac{mgR}{(I+mR^2)}\cos(\alpha_t+\theta) = \frac{\partial^2\alpha_t}{\partial t^2} \quad (1)$$

where T is the drag force required to initiate rolling, R is the radius of the particles (For a granular assembly with different particle sizes, d_{50} is used.), I is moment of inertia, which is equal to $mR^2/2$, m is the mass of the particle (for 2D, $m = \pi R^2 \rho_b$), ρ_b is the density of bed sediment particle, α_t is the angle between channel bed and connection line of centers of those two particles, θ is the slope angle, g is the gravity acceleration, $\partial^2\alpha_t/\partial t^2$—angular acceleration and t is time.

It is also assumed in the derivation that once the particle moves over the adjacent particle downstream, it will be considered to become part of flowing debris. Based on Eq. (1), the entrainment time, the time required for one particle to move from initial location into debris, can be calculated. The entrainment rate is defined as the height of particle exposed to the flow divided by the time needed for it to be eroded. Therefore for different α_0, the initial condition of α_t, entrainment rate, $\dot{E}_i$, is defined as:

$$\dot{E}_i = \frac{2R\sin\alpha_{0i}}{t_i} \quad (2)$$

t_i is the time required for one particle to roll from its initial position, α_0, to vertical line at which α_t equals $(\pi/2 - \theta)$, because it was assumed that once the particle moves over another particle, it will be considered as part of debris flow. Therefore, for a given shear force applied on the particle, t_i, can be determined from Eq. (1). When the shear force applied on the particle is larger than the friction at the particle contact, the entrainment mode changes from rolling motion to sliding motion.

Since α_0 varies considerably in the granular assembly and it is not easy to determine individual angles at each particle contact, a statistical approach is used to provide an estimate on the values and variations of α_0. It is assumed that the variation of α_0 can be approximated using a probability density function (PDF). The model parameters for a PDF have significant effects on the calculations of entrainment. Strictly speaking, parameters like mean value of normal distribution function would be possible to measure on site, but it only can apply to the site where the test was made. It can also be estimated using relationship between void ratio and internal friction angle, and relationship between particle protrusion and void ratio (Okada et al. 2007). The overall entrainment rate $\dot{E}$ can be determined from individual particle entrainment rate $\dot{E}_i$ and the probability density function P_i as:

$$\dot{E} = \sum_{i=1}^{n} (\dot{E}_i P_i) \tag{3}$$

where n is the number divisions of the probability density function in the approximation over the range of the values of α_0. For instance, if the increment of α_0 is 1 degree from 0 to 90 degree, n will be equal to 91.

3 Simulation

Although the debris flow surface velocities, runout distance and final volume can be observed in field and laboratory test, physical erosion process is still not easy to observe and shear stress existing on the erodible particles cannot be observed. It means that it is almost impossible to understand the erosion mechanism in particle scale based on conventional flume experiments. Therefore, Discrete Element Method becomes a good choice to understand the mechanism and explain the erosion process of granular particles. As one of discrete element method, PFC2D has the ability to monitor the kinematic characteristics of particles in built models. Since spherical particles with specified radius are used in the model, it can show idealized situation of physical flume experiments. In this way, other factors influencing the erosion process which include shape factor of the particles and particle size distribution of granular flow, can be excluded. Although the model simplifies real situation, it can still capture the main features of erosion process in granular flow. Moreover, since particles are rigid and have surface friction in PFC2D, erodible particles will be eroded one by one, which is consistent with progressive scouring mode instead of shear failure mode. Therefore, PFC2D is used to study erosion process in this study. Then the results will be used to verify the analytical entrainment model.

3.1 PFC used in debris flow study

Cundall [11] introduced a discrete element method to study rock-mechanics problems and then applied to soils by Cundall and Strack (1979). PFC2D model is developed using DEM, which is capable of describing the mechanical behaviours of assembles of particles by calculating the contact forces and displacements of each individual particle in response to its interaction with adjacent particles. Newton's second Law and force-displacement Law are used to calculate the motion of the particles. The assembly of particles continue to move until forces are in equilibrium or the mechanical energy has been completely dissipated by friction and/or system damping.

Banton [2] simulated channelized granular flows by considering the particle properties and basal surface properties. It was found that rebound coefficient between particles is important in the simulation when the flow is turbulent with a high velocity gradient. Three laboratory experiments, granular materials released from a rough inclined slope, carried out by Savage and Hutter [45] and Hutter et al. [19] were simulated. In the simulation, Banton [2] adopted spherical particles which could enhance the particle rolling and runout distance. The simulation results agreed with that observed very well, therefore it was suggested that DEM technique is able to simulate the physical process during channelized laboratory experiment of unigranular mass avalanches.

The dynamic response of colluvium accumulation slopes in Sichuan Province of China was studied by He et al. [15], since epicentre of Wenchuan earthquake occurred in 2008 is located in this region. The accumulations was considered as discontinuity in the simulation. Horizontal shearing waveforms of Wenchuan earthquake were used for the study of dynamic response. It was concluded that material properties and interface in the accumulation affected the velocity a lot.

Li et al. [27] and Montserrat et al. [38] simulated rapid movement and sudden failure of slope triggered by rainfall. Fluidization of the flowslide was simulated. Li et al. [27] found that residual friction coefficient is relatively important on the travel distance, height and location of debris flow fan. Moreover, geometry of slip surface had a great influence on the deformation of sliding mass. Montserrat et al. [38] found that finely grained flow moves longer that coarser flow and
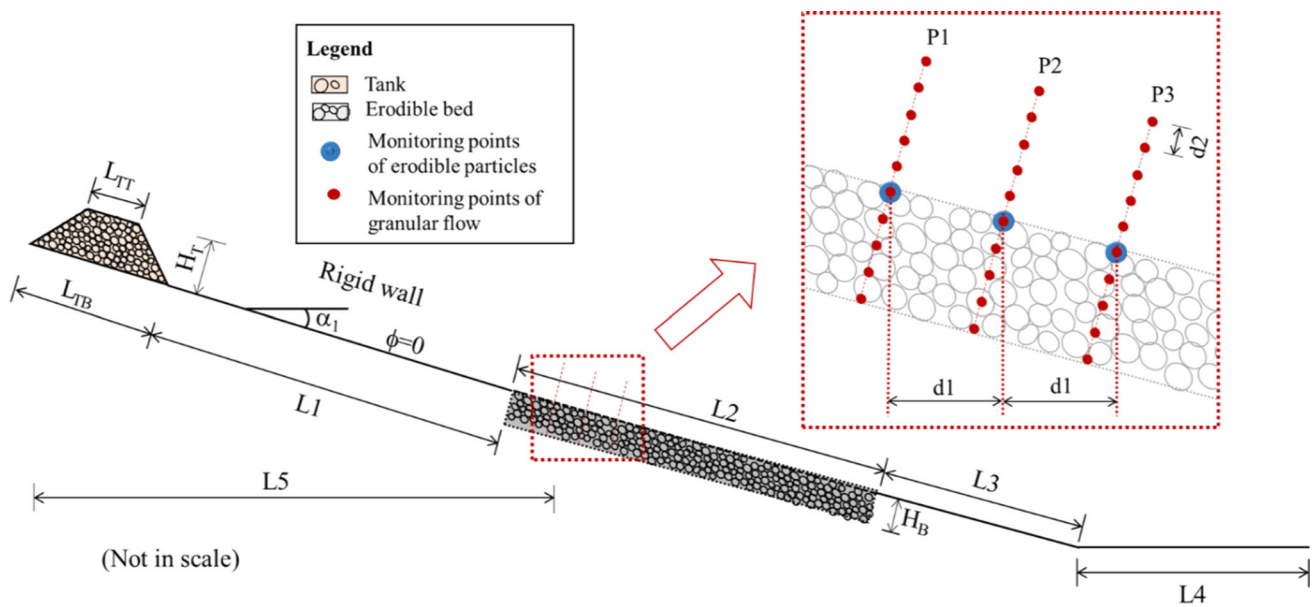
Fig. 2 Geometrical sketch of the idealized model considered in the study

fluidization could cause the increase of runout distance comparing with non-fluidized flow.

Effect of debris flow on barriers was tested using PFC2D [1,9,28,44]. A slope with constant inclined angle was constructed and a retaining wall was placed away from the toe of the slope. By varying the size of the retaining wall and particle properties, influence of geometry and particles properties was examined by measuring the impact force exerted on retaining wall. Zhou and Ng [50] also studied the reverse segregation in debris flow using flume experiments.

Crosta et al. [10] studied the debris flow characteristics based on FEM analysis. Slope angle and properties of channel bed were varied which include erodible and rigid beds. Kinematic characteristics are monitored in the simulations.

Though plenty of numerical flume experiments has been conducted, very few of them has taken entrainment into account in numerical flume experiment using PFC2D [16]. This paper aims to creatively analyze the entrainment using PFC2D. A flume with erodible bed is designed. Entrained volume, displacement and front velocity are monitored to test the availability of the new entrainment model.

3.2 Idealized model and geometry

To simulate the entrainment process, an idealized model with debris and erodible bed channel is constructed using PFC2D (Fig. 2). The model is mainly composed of three parts: acceleration section, erosional section and deposition section. The reason of using acceleration part is to provide enough kinetic energy when the particle reaches the erosional section. The erosional section, 0.15 m in depth, is the key part of this experiment, which consists of frictional particles with diameter ranging from 3 to 4 mm, the same as the particles in the tank. Finally, these particles are deposited as deposition zone. Since cohesionless particles are used here, parallel and contact bonds does not exist between them. Model parameters and material properties are summarized in Table 1.

3.3 Introduction on setting up PFC2D model

Based on the idealized model, flume experiments are carried out using PFC2D. Tank filled with particles is put at the top of channel. The depth of erosion is estimated by trial and error, since if erodible bed is too deep, this will significantly increase the computing time at each step and finally increase total calculation time. The horizontal length of erodible channel also needs to be set to an approximate value based on previous estimation.

Before generating the particles, walls used to simulate the rigid bed are generated first. Stiffness including shear stiffness and normal stiffness are larger than that of the particles to prevent particles from crossing the walls. As walls cannot overlap each other in PFC2D, overlapped wall used for generating erodible bed is deleted before putting the tank on the channel bed. Friction between the tank and the particles is assigned a smaller value. Otherwise, the particles at the bottom of the tank cannot slide into channel. In the simulation, frictionless wall is used for the bottom of the tank.

Particles are modelled as circular disks with unit thickness and filled the region enclosed by the walls. After preliminary equilibrium has been reach, walls covering the particles are removed. It is noted that the initial stress caused by compaction during the particle generation process should be released first, otherwise particles will move randomly with

Table 1 Geometrical parameters of the slope and tank

Parameters	Value	Parameters	Value
α_1 (°)	15	d1 (m)	0.2
L1 (m)	3	d2 (m)	0.0375
L2 (m)	2	LTT (m)	0.3
L3 (m)	3	LTB (m)	0.6
L4 (m)	2	HT (m)	0.3
L5 (m)	4	HB (m)	0.15
Particle size (m)	$0.003 \sim 0.004$	Density of particles (kg/m^3)	2600

high acceleration. Therefore particles need to be stabilized again. There may be some stresses built up at the toe of the slope, they do not significantly affect the simulation process as long as the particles remain unbounded [42]. The main body of the debris and the material in the erodible bed are represented by 5092 and 6392 particles, respectively with size ranging from 0.003 to 0.004 m. Since it is practically difficult to generate particles as much as in the actual debris flow, this number of particle in this simulation is acceptable.

The model is evaluated by examining the average velocity, total volume, rotational velocity and entrainment rate. Circular particles will roll and consequently a small number of particles will roll ahead and separate from the main body of the debris. In the simulation, if the particles move out of the right of deposition zone. The particles will not be considered as part of debris. The average velocity is defined as the average velocity of all moving particles. Variation of the average velocity means that moving mass encounters the slope having different friction coefficient. To calculate the change in volume, particles with displacement greater than a threshold value that is considered as about twice of mean particle size are assumed to be part of the flowing debris. Then, the volume of debris can be reckoned according to the number of mobilized particles and average porosity of the debris. Rotational velocities of the erodible and flowing particles are monitored using measurement circles in PFC2D.

3.4 Parameter settings in the PFC2D model

Using the DEM to simulate granular flow requires the determination of appropriate geometric and rheological parameters between the particles as well as for the basal surface [2]. Parameters used in the numerical experiment are shown in Table 2.

In determining the model parameters, interparticle bonding strength are set to be zero since only rolling motion is considered in the model. By default, the friction coefficient at the ball-wall contacts equals the minimum friction coefficient of the ball and the wall. Since Mangeney et al. [31] and Iverson et al. [21] used the same material for the source and erodible material in the laboratory and field experiments,

Table 2 Parameter setup in modelling (for channel bed and tank)

Items	Microscopic mechanical parameters of PFC model
Particle size	
Maximum radius (m)	0.004
Minimum radius (m)	0.003
PDF	Uniform distribution
Particle density (kg/m^3)	2600
Porosity	0.2
Particle normal stiffness (N/m)	1e9
Particle shear stiffness (N/m)	1e9
Contact bond normal and shear strengths	0
Ball-ball friction	0.6
Ball normal stiffness (N/m)	1e10
Ball shear stiffness (N/m)	1e10
dt scale	1e-5
Local damping coefficient	0
Viscous damping coefficient (normal)	0.3
Viscous damping coefficient (shear)	0

respectively, the particles in the main body of the debris and in the erodible bed have the same properties in this simulation including porosity, particle size distribution, etc. since they are essentially the same material. To prevent particle from flying away after removing the wall what was used in the particles generation, the velocities of the particles are set to zero after each calculation loop in the initial stage.

Local and viscous damping are used to dissipate kinetic energy in order to arrive a steady state solution in a reasonable number of cycles. Local damping is used to apply damping force to each ball or clump (collection of particles) with magnitude proportional to the unbalanced force. Instead, viscous damping is applied at the contact by imposing normal and shear forces at each contact directly proportional to the relative velocities at the contact. The default values for local and viscous damping ratio are 0.7 and 0, respectively [20].

Local damping

$$F_{(i)} + F^d_{(i)} = m_{(i)}a_{(i)}; \quad i = 1, 2, 3 \tag{4}$$

where $F_{(i)}$, $m_{(i)}$ and $a_{(i)}$ are the generalized force, mass and acceleration components, respectively; F_i includes contribution from gravity force; and $F^d_{(i)}$ is the damping force which is given by:

$$F^d_{(i)} = -\alpha \left| F_{(i)} \right| \operatorname{sign} \left(v_{(i)} \right) \tag{5}$$

where α is local damping coefficient and v is the generalized velocity.

$$v_{(i)} = \begin{cases} \dot{x}_{(i)}, & for\ i = 1, 2 \\ \dot{\omega}_{(i)}, & for\ i = 3 \end{cases} \tag{6}$$

$$\operatorname{sign}(y) = \begin{cases} +1, & if\ y > 0 \\ -1, & if\ y < 0 \\ 0, & if\ y = 0 \end{cases} \tag{7}$$

In calculating viscous damping, normal and shear components of a damping force are given by

$$D_i = c_i \left| v_i \right| \tag{8}$$

where c_i is the damping constants, V_i is the relative velocity at the contact, and the subscript i refers to one of the two components of the contact force ($i = 1$ means normal force, and $i = 2$ shear force). Instead of specifying the damping constants, the critical damping constant is specified. The relationship between damping constant, c_i, and critical damping constant is

$$c_i = \beta_i c_i^{crit} \tag{9}$$

where β is critical damping ratio. When $\beta < 1$, the system is said to be underdamped or lightly damped; when $\beta > 1$, the system is said to be overdamped or heavily damped. c^{crit} is the critical damping constant, which is given by

$$c_i^{crit} = 2m\omega_i = 2\sqrt{mk_i} \tag{10}$$

where ω_i is the natural frequency of the undamped system, k_i is the contact tangent stiffness and m is the effective system mass.

4 Simulation results

To test the effects of entrainment on debris flow runout, particles located as specified coordinate are monitored (Fig. 2). Runout distance and velocity of debris flow are obtained by monitoring moving and stationary particles in the flow channel. 30 locations, distributed evenly in three cross sections, are being monitoring. Shear stresses inside the measurement circles are monitored. To obtain entrainment rate dynamically, stresses and variations of the height at the interface

between moving and stationary particles are calculated. Figure 3 shows the locations of flowing particles at different time. Since entrainment starts when the moving particles reaches the erodible bed, the authors analyze the depth of erosion caused by moving particles.

4.1 Average velocity and total volume

During the simulation process, average velocity and total volume are calculated. Average velocity is calculated based on all moving particles. Total volume is defined as the volume of all particles mobilized. Figure 4 indicates the calculated velocity and total volume. The average velocity increases linearly until the moving particles reach the erodible bed. The maximum velocity, around 2.10 m/s, occurs at the beginning of entrainment process. After that, the average velocity decreases continuously until $t = 4.5$ s. Variation of the total volume of the moving particles starts at $t = 3.2$ s. Therefore, analysis of simulation results will focus on the velocities and total volume in the shaded region, between $t = 3.2$ s and $t = 4$ s, as shown in in Fig. 4.

4.2 Rotational velocities

Lin and Wu [29] suggested a method to average the rotational velocity of particles. This study focuses on the interface between moving particles and stable channel bed, which thickness is approximately equal to the diameter of the particle. Corresponding to the method proposed by Lin and Wu [29], the radius of the average circle should be smaller than the radius of particle size, resulting in that the average rotation velocity is equal to the particle rotation velocity. Therefore, the particle rotation velocities are plotted.

Figure 5 shows the calculated rotational velocity of the particles closest to monitoring points at the erodible channel surface. These particle are selected at the initial stage of the numerical experiment and the rotational velocities are tracked throughout the flow process. Physically, particles closest to the surface of the erodible channel at P1 are moved first and then particles at P2 and P3 are moved consecutively. Positive value indicates counterclockwise rotation according to the default setting in PFC2D. The time when particles start to rotate agrees with the time when erosion starts. It means that the rotational velocities correspond with physical analysis though negative rotational velocities observed that are probably caused by particles climbing over the monitored particles.

4.3 Properties measured using measurement circles

In PFC2D, contact forces and particle displacements are calculated at the micro level. Since they cannot be compared directly to a continuum model, averaging procedures are used

Fig. 3 Dynamic location of moving granular flow and close up of measurement circles
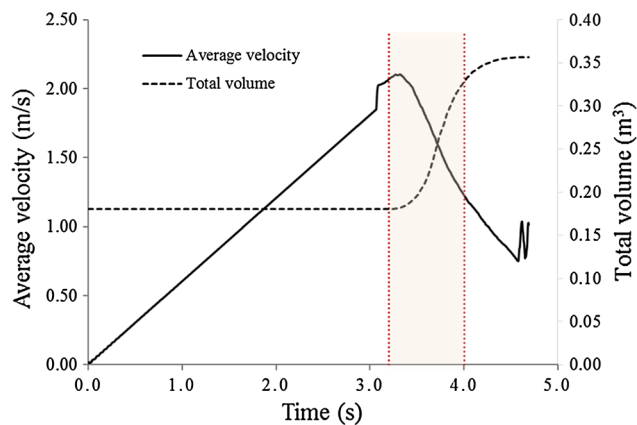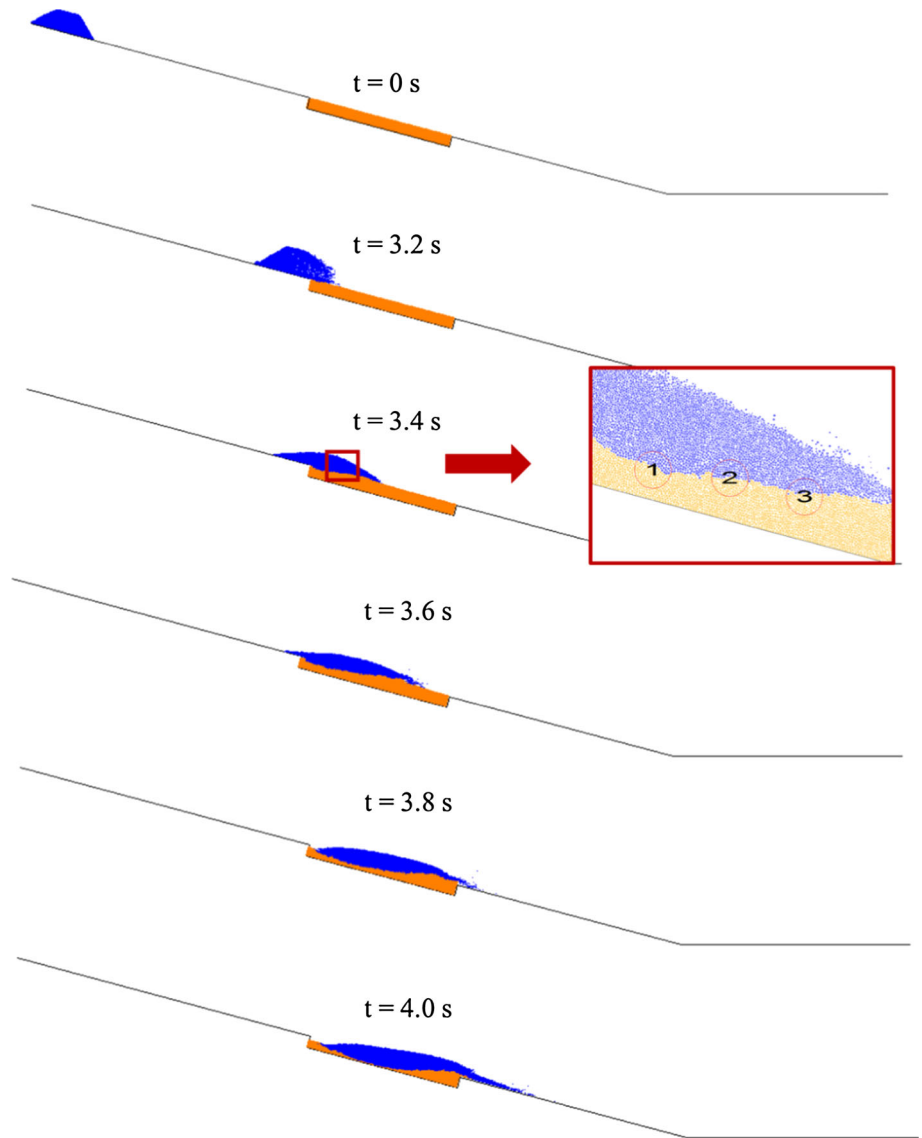
**Fig. 4** Average velocity of moving particles

to calculate macro stresses. The average stress tensor, $\bar{\sigma}_{ij}$, in a volume V of material, is defined as:

$$\bar{\sigma}_{ij} = \frac{1}{V} \int_V \sigma_{ij} dV \qquad (11)$$

where $\bar{\sigma}_{ij}$ is the stress acting throughout the volume V.

According to contact forces, contact orientations and region porosity, the average stress tensor, $\bar{\sigma}_{ij}$, is estimated using stress-measurement procedure developed by Potyondy and Cundall [40]. In the estimation, it is assumed that there is no body force and particles satisfy full-force equilibrium and parallel-moment equilibrium is not satisfied. Outward normal stress is considered as positive value. Force per unit length of particle boundary are converted to a stress quantity by dividing the force by the thickness of the element. Since
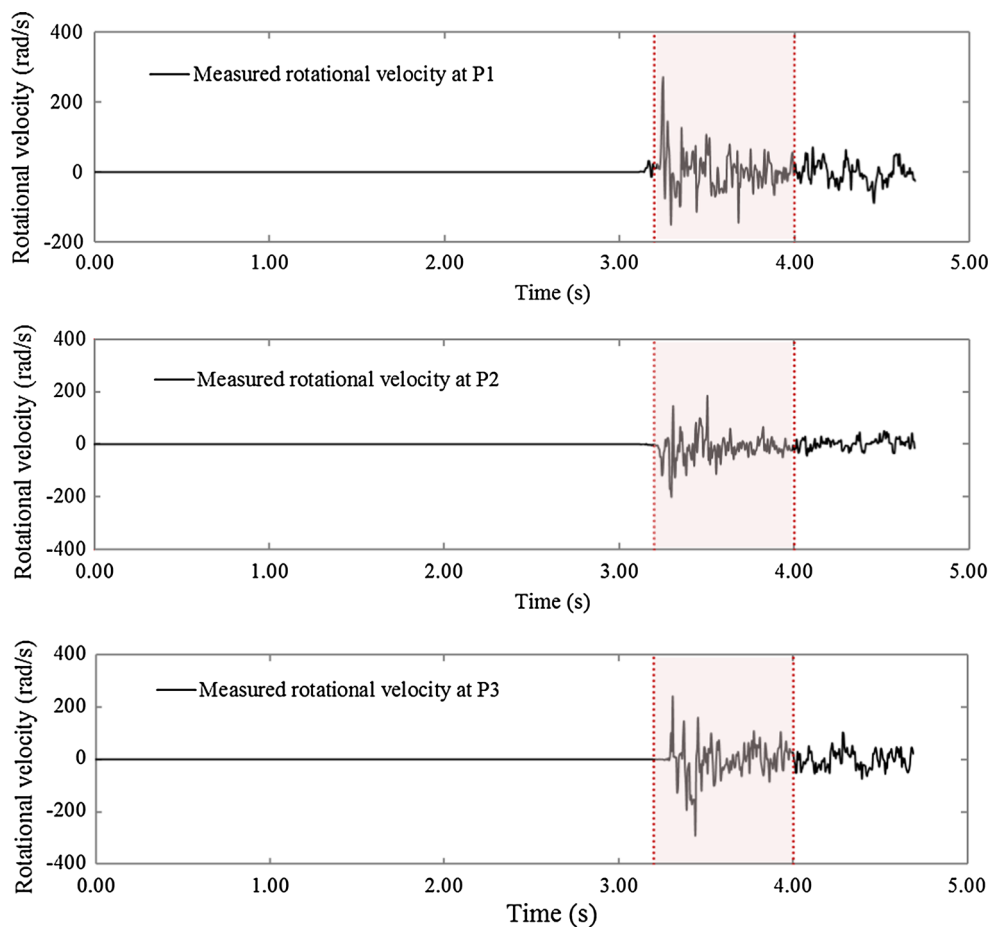
Fig. 5 Variation of rotational velocities of particles at monitoring points

shear stress along the flow channel is needed, stress transformation is necessary after calculating the normal and shear stresses (Fig. 6).

The size of measurement circle can affect the calculated values. To see the effect of the size of measurement, various sizes are used in the calculation of the shear stresses. The results are plotted in Fig. 7. It is obvious that the shear stress converges to a single value if the size of the measurement circle increases.

Figure 8 shows the distribution of x-velocity, rotational velocity and shear stress in the granular flow during the flowing process along the cross sections. Since friction dominates the properties of granular flow, which is different from viscous flow in which viscosity dominates the flow properties, the largest x-velocity appears at the top of the flow channel, notably at B1 and C1. At A1, due to boundary effect, x-velocity of particles near the initial erodible surface is smaller than that below the initial erodible surface, however in B1 and C1, the calculated x-velocity is almost linearly distributed similar as simple Couette flow.

Rotational velocity at the monitored sections varies considerably between positive and negative values with depth.

Since particles override each other, underlying particles requires larger force to be moved than the particles above. When the upper particle roll forward, counter clockwise rotation, the lower particles then roll backward, clockwise rotation, due to friction at the contact. This results in rapid changes in the direction of rotation between positive and negative values with depth.

Shear stresses also vary along the cross sections. However shear stresses are increasing from top to bottom in the moving particles. Since stresses are calculated using average values in a volume depending on porosity, it is expected that shear stresses will vary a little bit along the cross sections.

(A-1, B-1 and C-1 are monitored x-velocity along cross sections P1, P2 and P3. A-2, B-2 and C-2 are monitored rotational velocity along cross sections P1, P2 and P3. A-3, B-3 and C-3 are monitored shear stress along cross sections P1, P2 and P3, which have been transformed to the direction parallel to flow channel).
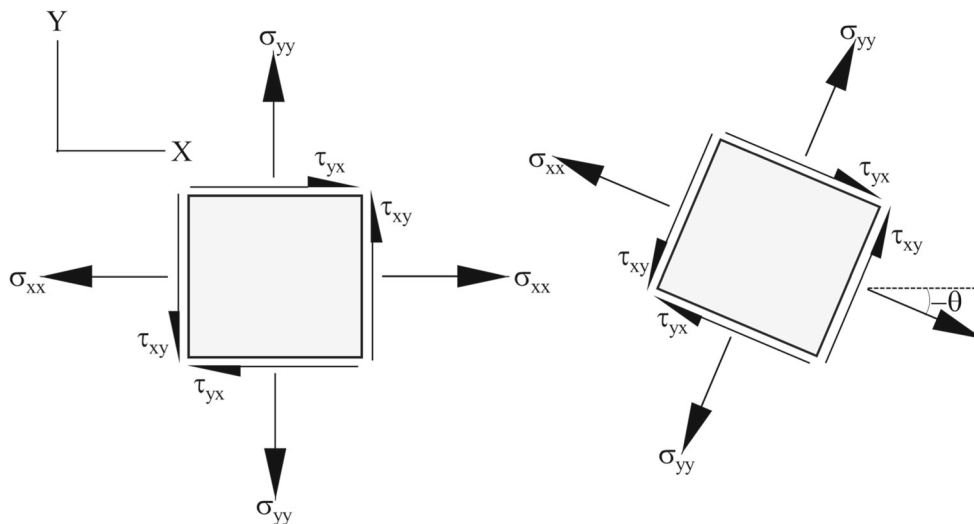
Fig. 6 Stress transformation during to slope of the erodible bed
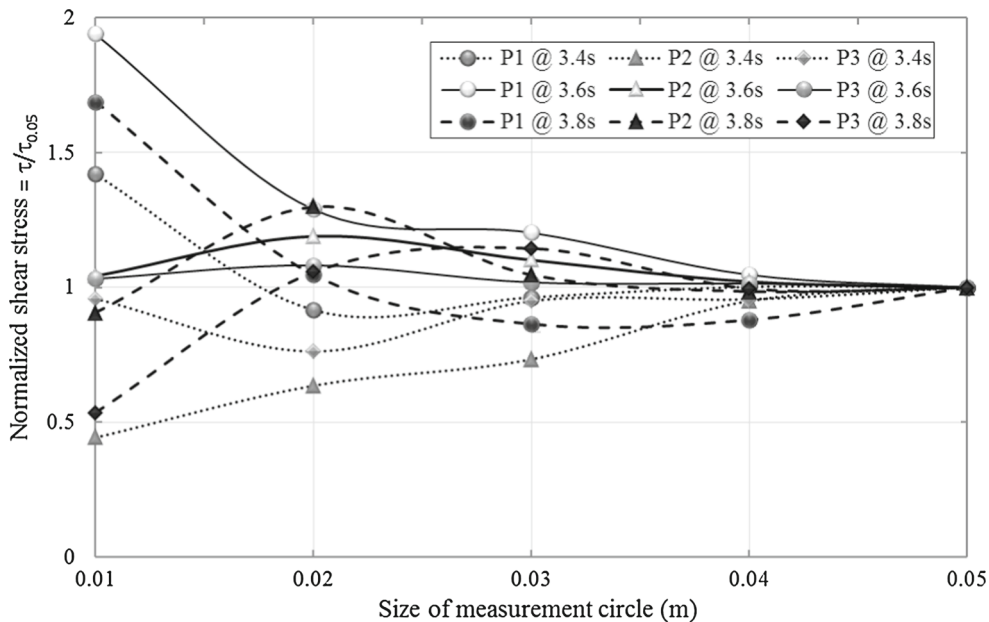

Fig. 7 Sensitivity test of the size of measurement circle on shear stress

5 Calculation using the analytical model and results comparison

To verify the analytical model, the rate of erosion is also calculated using the analytical model. Parameters in the analytical model is selected based on the parameters used in numerical experiments. Detailed information regarding parameter selection is as follows.

5.1 Parameter selection

The value of α_0 cannot be easy measured in the field. However it is shown that α_0 can be related to a pivoting angle. In the simulation, pivoting angle of angular particle, ϕ_p, is estimated using the empirical relationship from Li and Komar (1986). The average slope angle is used here. The mean value of the normal distribution PDF is calculated to be 33° based on the relationship that $\alpha_0 = (\pi/2 - \phi_p)$. A standard deviation value equal to 0.1 is used. The average particle size, 3.5 mm, used in the PFC simulation is also used in the analytical model. The particle density used in the calculation is the same as that used in the PDF simulation.

The contact friction angle, ϕ_μ, is not the same as the aggregate angle of friction ϕ_{cv} at critical state. Caquot [6] related ϕ_μ and ϕ_{cv} using:
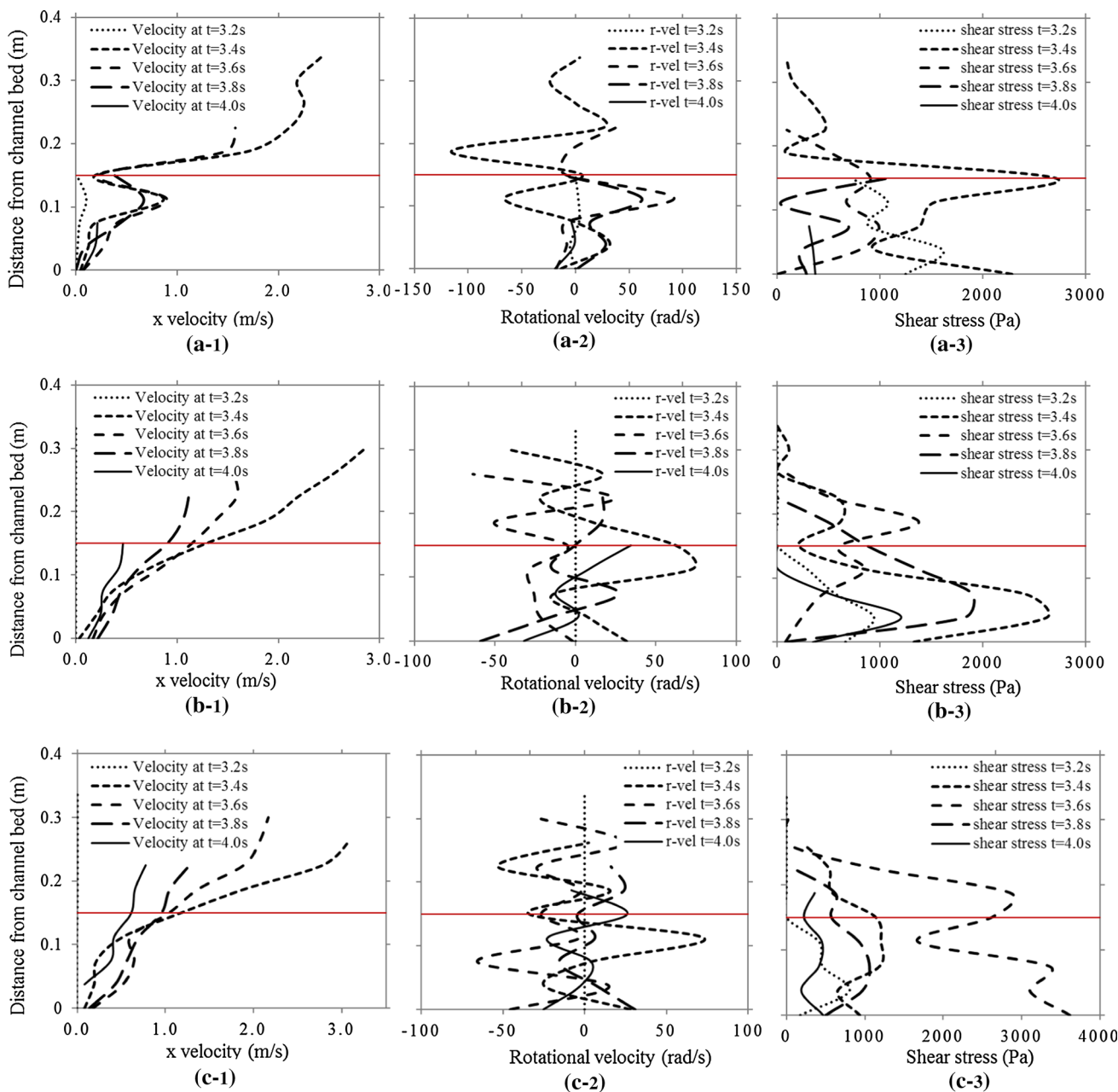
Fig. 8 Flow properties along monitored cross sections

$$\tan \phi_{cv} = \frac{1}{2}\pi \tan \phi_{\mu} \tag{12}$$

Bishop [4] also developed an approximate solution verified using double measured values ϕ_{μ} and ϕ_{cv}.

$$\sin \phi_{cv} = \frac{15 \tan \phi_{\mu}}{10 + 3 \tan \phi_{\mu}} \tag{13}$$

In the calculating entrainment, Eq. (12) is used to relate the friction angle in PFC simulation to the friction angle in the probabilistic entrainment model. According to the friction

angle in PFC simulation, an internal frictional angle is calculated based on the equation above which will be equal to the mean value of PDF in probabilistic entrainment model. Standard deviation equal to 0.01 is used in the calculation.

5.2 Verification of calculated shear stress

To evaluate the new entrainment model, shear stress, variation of erodible depth and entrainment rate are compared with the results from PFC numerical experiment along sections P1, P2 and P3. Shear stress is defined as the stress always

along the slope. Shear stresses at the interfaces between the granular flow and the immobile particles are compared to that calculated using the Coulomb friction model and the Voellmy fluid model in the runout model (Fig. 9). The height of the flowing particles used in calculating the shear stresses in the Coulomb friction model and the Voellmy fluid model is measured at a 0.05 s interval in the entrainment process in PFC2D. In shear stress calculation, the turbulence coefficient in the Voellmy fluid model is equal to 100 m/ s^2 which is selected based on the suggestion of Luna et al. [30].

The component representing normal stresses in Coulomb friction model and Voellmy fluid model is obtained from the measurement circles by stress transformation. The friction coefficient and turbulent coefficient are selected as mentioned above. The shear stress then can be calculated using the Coulomb friction model and Voellmy fluid model. The component representing shear stress along slope in PFC experiment can also be obtained by stress transformation according to the stresses calculated using measurement circles. Figure 9 shows there are discrepancies between calculations from PFC model and the constitutive models. The shear stress from PFC model matches that estimated using the Voellmy fluid model initially. However, at a later stage, the PFC calculated shear stress is closer to the stresses calculated using the Coulomb friction model.

5.3 Verification of the depth of erosion

To evaluate the new entrainment model, variation of the depth of erosion and entrainment rate are compared with the results from PFC numerical experiment at sections P1, P2 and P3. The entrainment depth or the depth of erosion in the PFC experiment is defined as the depth of the particles in the erodible zone which have been mobilized and subsequently including in the flowing granular material. Figure 10a–c show that entrainment starts until the moving particles reach erodible zone and entrainments almost stop if the moving particles reach the rigid boundary (channel bed), considered as not erodible. Besides the depths of erosion calculated using the progressive model and PFC2D model in which particles are free to rotate, static and dynamic analytical models along with PFC2D models in which only sliding motion is allowed, are also used to calculate the depths of erosion.

The static and dynamic entrainment equation proposed by Medina et al. [36] are initially considered for erosion calculation. Both of them are used to compare with the depths of erosion calculated using PFC2D model (rolling motion). The static model is independent of the calculation time step. By comparison, the dynamic model can provide the variation of the rate of erosion. The static model calculates the depth of erosion based on the equilibrium of erodible soil showing below.

$$h_{ent} = \frac{(\tau_b - \tau_{res})}{\rho g (\cos\theta \tan\varphi_{bed} - \sin\theta)} \tag{14}$$

where h$_{ent}$ is the depth of erosion, τ_b is the shear stress applied to the channel bed, τ_{res} is basal resistance, ρ is the bulk density of debris, g is gravity acceleration, θ is slope angle, and ϕ_{bed} is the friction angle of bed material.

The dynamic entrainment equation is used to calculate the entrainment rate that is positively correlated with net driving force, given by

$$\frac{\partial z}{\partial t} = \frac{1}{\rho V_{ave}}(\tau_b - \tau_{res}) \tag{15}$$

where $\partial z/\partial t$ is the rate of erosion, and V_{ave} is the mean velocity of moving particles.

In PFC simulations with rolling motion, the accumulated depth of erosion at specific locations is obtained from the observation of the depth of eroded particles. This is the same for the simulation of entrainment process using dynamic model in which rolling motion is limited. For the simulation of the static model, the accumulated depth is obtained through the comparison of shear stress at the bed of moving particle and the shear resistance along the depth of erodible bed, where the stress cannot overcome the resistance. The shear stress and resistance are calculated from the PFC simulation at different time stage.

In the calculation of the depth of erosion using analytical models, the shear stresses at the interface between moving particle and stable bed are calculated using PFC models. For the progressive scouring model, the depth of erosion is calculated using the progressive model based on the parameters listed in Table 2. For the dynamic model, the shear resistance is calculated based on Mohr–Coulomb frictional model, equal to the normal stress from calculation in PFC multiplies frictional coefficient. In the static and dynamic models, bulk density is calculated according to the density of the particles and void ratio when particles are generated, which is equal to 2080 kg/m^3. Basal friction angle is modified using equation [12], equal to 43°. Slope angle is the same as the in the model, 15°. g is equal to 9.81 m/s^2.

Figure 10 shows that the depths of erosion estimated using the progressively model agree well with that determined at P1, P2 and P3 until time equals to $t = 3.8$ s at which time the moving particles reach the rigid wall. When moving particles reach this boundary, the interface will not change any more no matter what is the magnitude of shear stress applied on channel bed. The discrepancies after $t = 3.8$ s are mainly caused by the reason mentioned above. It means after $t = 3.8$ s, although the shear stress calculated in PFC is not equal to zero, the entrainment rate should be equal to zero. However, this discrepancy is not large as the moving particles fully stop less than 0.2 s later.

Fig. 9 Shear stress measured and calculated at interface between moving particle and immobile particles. **a**, **b** and **c** are comparison results from P1 to P3, respectively

(a)

(b)

(c)
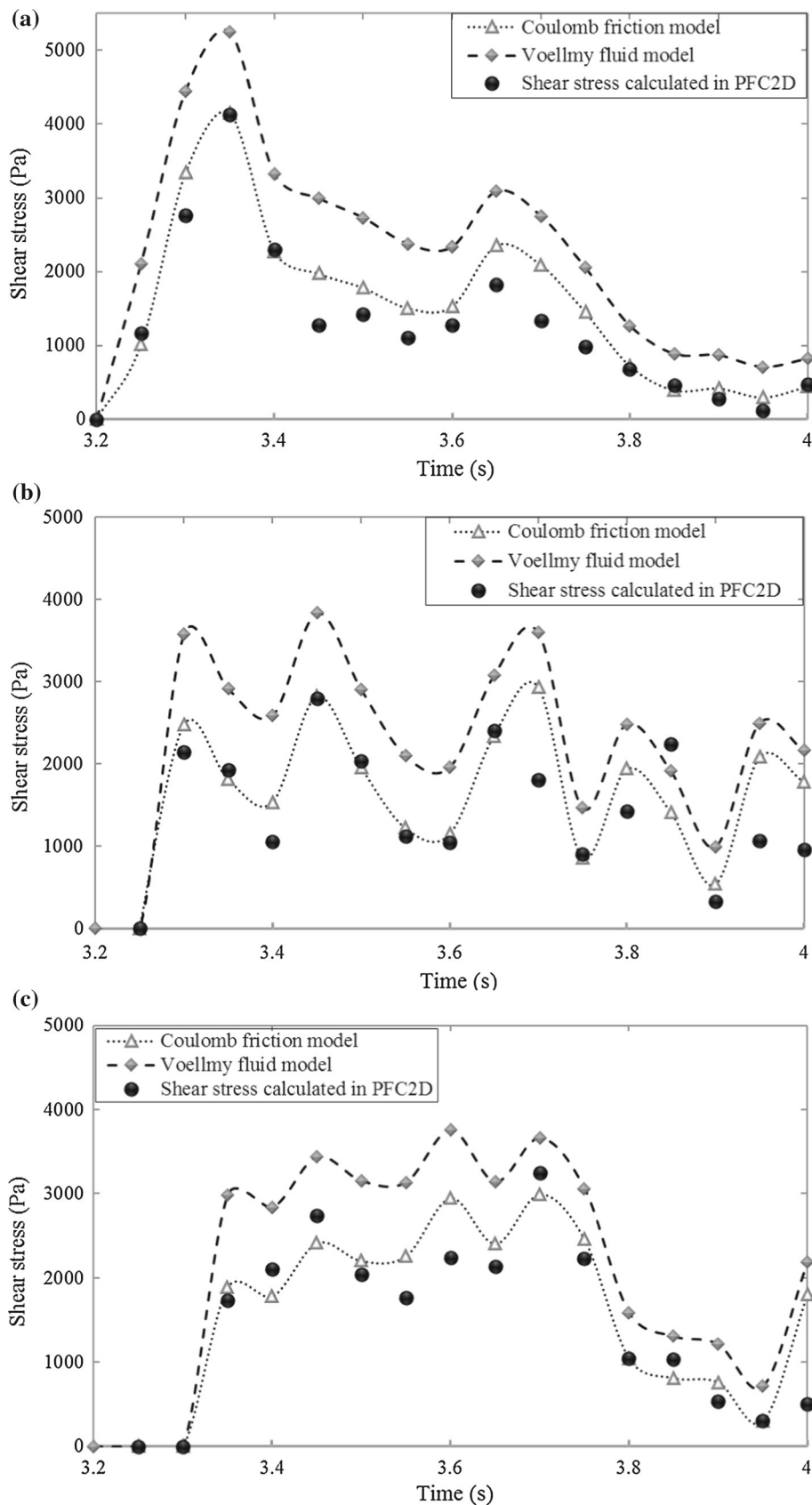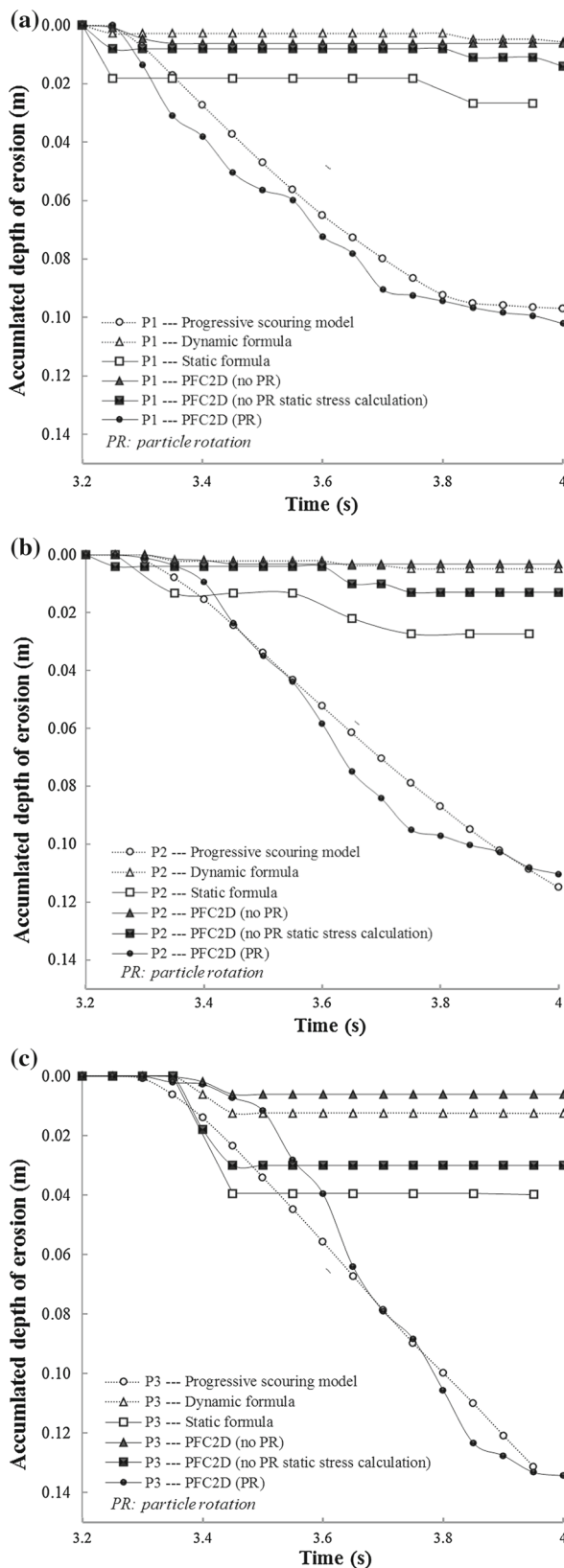
Fig. 10 Comparison of analytical and PFC2D simulated depth of erosion. **a** Comparison of the accumulated depth of erosion at P1, **b** comparison of the accumulated depth of erosion at P2 and **c** comparison of the accumulated depth of erosion at P3
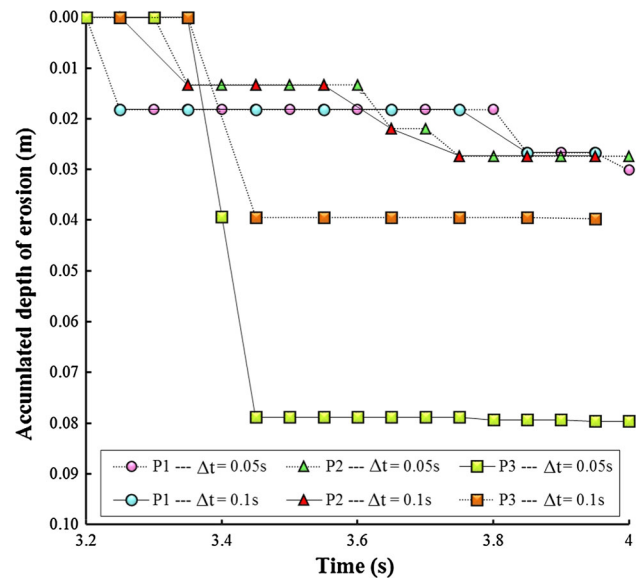
Fig. 11 Calculated depth of erosion using static formula under different time steps

In PFC2D, if the particles are restricted from rolling, final the depth of erosion from static and dynamic models are smaller than that from rolling motion such as static and dynamic results in PFC2D. It means that neglecting the rolling motion in entrainment calculation could lead to the underestimation of erosion depth.

The differences of entrainment depths between calculated values using the dynamic model and the progressive scouring model and that calculated in PFC experiments, are presented using the values of mean square error (MSE) which indicated the average of the squares of the errors.

$$MSE = \frac{1}{n}(\hat{Y}_i - Y_i)^2 \qquad (16)$$

where n is the number of predictions, $\hat{Y}_i$ is the observed value, and Y_i is the predicted value.

MSE of calculated depth of erosion using different entrainment models and the depth of erosion from the numerical experiment are shown in Table 3. It is obvious that the depth of erosion calculated using the progressive scouring model are closer to the calculated depth of from the PFC model. Although it seems that static formula performs better than the dynamic formula, it is easily effected by the time step in the calculation.

Figure 11 indicates the accumulated depth of erosion calculated using static formula. When time step increases from 0.05 to 0.1 s, theoretically, the depth of erosion will be smaller indicated at P3. Even though the final depth of erosions at P1 and P2 when $\Delta t = 0.1$ s are the same as that when $\Delta t = 0.05$ s, the rate of erosion is smaller when $\Delta t = 0.1$ s at $t = 3.8$ s for P1 and at $t = 3.6$ s and $t = 3.7$ s for P2.

Table 3 MSEs of calculated entrainment depths between static, dynamic entrainment models and PFC experiment (rolling)

Entrainment models	P1	P2	P3
Progressive scouring model (m^2)	0.00005	0.00005	0.00011
Dynamic formula (m^2)	0.00475	0.00443	0.00456
Static formula (m^2)	0.00290	0.00260	0.00250
PFC2D (no PR) (m^2)	0.00444	0.00409	0.00518
PFC2D (no PR static stress calculation) (m^2)	0.00408	0.00374	0.00315
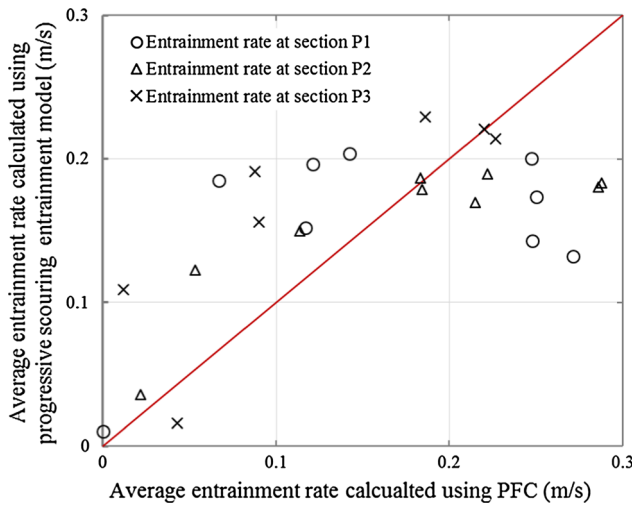
Fig. 12 Comparison of entrainment rate between progressive entrainment model and PFC2D simulation

5.4 Verification of the rate of erosion

The rate of erosion is calculated by dividing the depth of erosion by the time. The new entrainment model is verified by comparing the entrainment rate between progressive scouring model and the PFC results. Figure 12 indicates the entrainment rates calculated using the progressive scouring model and using PFC. The deviation of entrainment rate calculated can be explained by the errors in identifying the erosion depth in discrete model which is different from continuous model.

The calculated entrainment rate from the progressive scouring entrainment model at P1 varies between 0.13 and 0.21 m/s, while the entrainment rates of the other two lines change almost evenly along the diagonal line. By monitoring the entrainment process at P1, it is found that the boundary effect affects the entrainment calculation since the height of moving mass is probably overestimated which is used to calculate the shear stress in the progressive scouring entrainment model. It is because some of the particles at the top part of the flow are not fully contacted with underlying particles in PFC model. These particles do not develop shear stress on the flow channel.

6 Discussion

The height of the erodible channel is critical in the experiments. The erodible part can be neither too shallow, since it will be eroded to a rigid wall quickly, and nor too deep, as it will then need more calculation time at each step. Therefore, calculation time and visible entrainment process should be balanced. Moreover, to prevent the flying the particles, stiffness of particles in the tank and erodible channel should be set as a small value before overlapping of particles is observed at the bottom part of the erodible channel.

Since it is assumed that rolling motion is the main process in the progressive scouring entrainment model, rotational velocities of the particles located at three different cross sections are monitored. Observed results indicate that rotational velocities at the monitoring spots suddenly increase when entrainment starts which indicates that the rolling motion is an essential part in entrainment process and should be incorporated into the entrainment process with sliding motion. A change of rotational velocity between positive and negative values is induced by the interaction between adjacent rigid particles and/or particle and wall.

The shear stresses applied on channel bed are calculated in PFC using measurement circles based on stress transformation. The stresses perpendicular to the slope which are also calculated using measurement circles in PFC are used to calculate shear stress adopting Mohr–Coulomb friction model and Voellmy fluid model. The results indicate that the shear stresses calculated using Mohr–Coulomb friction model are closer to that calculated using PFC. In stress monitoring, size of measurement circle could impact the measured stress although the difference is very small.

The rate of erosion in PFC simulation is obtained by observing the variation of the depth of erosion of mobilized particles. The rate of erosion is also calculated using progressive scouring model and dynamic entrainment model. The parameters in the progressive scouring model is selected based on the parameters in the PFC including density, internal friction angle, and mean value of particle size. The comparison result of the variation of the depth of ero-

sion demonstrates that the erosion process mainly occurs between 3.3 and 3.7 s. The erosion depths are also calculated using PFC models with and without rolling motion, the static and dynamic entrainment formulas and the progressive scouring entrainment model. The calculated depths of erosion using the progressive scouring entrainment model and the static and dynamic formulas indicate omitting the rolling motion in entrainment calculation could lead to the underestimation of entrainment. Therefore, in future erosion calculation, rolling motion and sliding motion are all needed to be incorporated in entrainment calculation. In addition, for static formula, time step is very important which has been demonstrated in Fig. 11. Therefore, timing effect should be taken into consideration which has been incorporated in the dynamic formula and progressive scouring model. The scatter plot substantiates that it is feasible to use the progressive scouring entrainment model to estimate the entrainment rate, in which rolling motion starts first.

7 Conclusion

The analytical model considers that the rolling motion dominants the erosion process of loose packed granular particles. Since the arrangement of particles is random which leads the difficulty in determining the α_0, PDF is used and mean value of α_0 is calculated according to the pivoting angle of particles which can be related to the diameter of particles based on an empirical relation.

PFC2D has the ability to capture the entrainment process of granular flow. The advantage of numerical experiment is that it can calculate the shear stress during debris flow movement which is really difficult or even impossible so far in field and laboratory tests.

Monitoring results indicate that the rolling motion occurs when entrainment starts. The calculated depth of erosion using the progressive scouring model is closer to the actually measured depth comparing with that calculated using the static and dynamic formulas, showing that only considering shear failure motion in erosion calculation could cause the underestimation of erosion depth.

Compliance with ethical standards

Conflict of interest We declare that we have no financial and personal relationships with other people or organizations that can inappropriately influence our work, there is no professional or other personal interest of any nature or kind in any product, service and/or company that could be construed as influencing the position presented in, or the review of, the manuscript entitled.

References

1. Albaba, A., Lambert, S., Nicot, F., Chareyre, B.: Relation between microstructure and loading applied by a granular flow to a rigid wall using DEM modeling. Granul. Matter **17**(5), 603–616 (2015)
2. Banton, J., Villard, P., Jongmans, D., Scavia, C.: Two-dimensional discrete element models of debris avalanches: parameterization and the reproducibility of experimental results. J. Geophys. Res. **114**, F04013 (2009). https://doi.org/10.1029/2008JF001161
3. Berger, C., McArdell, B.W., Schlunegger, F.: Direct measurement of channel erosion by debris flows, Illgraben, Switzerland. J. Geophys. Res. Earth Surf. **116**(F01002) (2011). https://doi.org/10.1029/2010JF001722
4. Bishop, A.W.: Correspondence. Géotechnique **4**(1), 43–45 (1954)
5. Bouchut, F., Ionescu, I.R., Mangeney, A.: An analytic approach for the evolution of the static/flowing interface in viscoplastic granular flows. Commun. Math. Sci. **14**(8), 2101–2126 (2016)
6. Caquot, A.: Equilibre des Massifs a' Frottement Interne. Stabilite des Terres Pulv6rents et Coherentes. Gauthier Villars, Paris (1934)
7. Cheng, N.S., Law, A.W.K., Lim, S.Y.: Probability distribution of bed particle instability. Adv. Water Resour. **26**(4), 427–433 (2003)
8. Chigira, M.: Dry debris flow of pyroclastic fall deposits triggered by the 1978 Izu-Oshima-Kinkai earthquake: the "collapsing" landslide at Nanamawari, Mitaka-Iriya, southern Izu Peninsula. Nat. Disaster Sci. **4**(2), 1–32 (1982)
9. Chou, S.H., Lu, L.S., Hsiau, S.S.: DEM simulation of oblique shocks in gravity-driven granular flows with wedge obstacles. Granul. Matter **14**(6), 719–732 (2012)
10. Crosta, G.B., Imposimato, S., Roddeman, D.: Granular flows on erodible and non erodible inclines. Granul. Matter **17**(5), 667–685 (2015)
11. Cundall, P.A.: A computer model for simulating progressive, large scale movements in blocky rock systems. In: Proceedings of the International Symposium on Rock Mechanics, Editors: Anonymous, Nancy, France, October 4–6, 1971, vol. 2, pp. 129–136. Rubrecht, Germany (1971)
12. Cundall, P.A., Strack, O.D.: A discrete numerical model for granular assemblies. Géotechnique **29**(1), 47–65 (1979)
13. Egashira, S., Honda, N., Itoh, T.: Experimental study on the entrainment of bed material into debris flow. Phys. Chem. Earth Part C Sol. Terr. Planet. Sci. **26**(9), 645–650 (2001)
14. Fenton, J.D., Abbott, J.E.: Initial movement of grains on a stream bed: the effect of relative protrusion. Proc. R. Soc. Lond. Ser. A Math. Phys. Eng. Sci. **352**(1671), 523–537 (1977)
15. He, J.M., Li, X., Li, S.D., Yin, Y.P., Qian, H.T.: Study of seismic response of colluvium accumulation slope by particle flow code. Granul. Matter **12**(5), 483–490 (2010)
16. Higashitani, K., Iimura, K., Harota, M., Suzuki, M., Watanabe, S.: Simulation of entrainment of agglomerates from plate surfaces by shear flows. Chem. Eng.Sci. **64**(7), 1455–1461 (2009)
17. Hungr, O., Evans, S.G.: Entrainment of debris in rock avalanches: an analysis of a long run-out mechanism. Geol. Soc. Am. Bull. **116**(9–10), 1240–1252 (2004)
18. Hungr, O., Leroueil, S., Picarelli, L.: The Varnes classification of landslide types, an update. Landslides **11**(2), 167–194 (2014)
19. Hutter, K., Koch, T., Plüss, C., Savage, S.B.: The dynamics of avalanches of granular-materials from initiation to runout. 2. Experiments. Acta Mech. **109**(1–4), 127–165 (1995)
20. Itasca, Consulting Group Inc., PFC2D Particle Flow Code in 2 Dimensions. User's Guide (2002)
21. Iverson, R.M., Logan, M., LaHusen, R.G., Berti, M.: The perfect debris flow? Aggregated results from 28 large-scale experiments. J. Geophys. Res. Earth Surf. **115**(F03005), (2010). https://doi.org/10.1029/2009JF001514

22. Iverson, R.M., Reid, M.E., Logan, M., LaHusen, R.G., Godt, J.W., Griswold, J.P.: Positive feedback and momentum growth during debris-flow entrainment of wet bed sediment. Nat. Geosci. **4**(2), 116–121 (2011)

23. Iverson, R.M.: Elementary theory of bed-sediment entrainment by debris flows and avalanches. J. Geophys. Res. **117**(F03006) (2012). https://doi.org/10.1029/2011JF002189

24. Iverson, R.M., Ouyang, C.: Entrainment of bed material by Earth-surface mass flows: review and reformulation of depth-integrated theory. Rev. Geophys. **53**(1), 27–58 (2015)

25. Kang, C., Chan, D., Su, F., Cui, P.: Runout and entrainment analysis of an extremely large rock avalanche—a case study of Yigong, Tibet, China. Landslides **14**(1), 123–139 (2017)

26. Kang, C., Chan, D.: Modelling of entrainment in debris flow analysis for dry granular material. Int. J. Geomech. (ASCE) **17**, 04017087 (2017)

27. Li, W.C., Li, H.J., Dai, F.C., Lee, L.M.: Discrete element modeling of a rainfall-induced flowslide. Eng. Geol. Eng. Geol. **149**, 22–34 (2012)

28. Li, X.P., He, S.M., Luo, Y., Wu, Y.: Discrete element modeling of debris avalanche impact on retaining walls. J. Mt. Sci. **7**(3), 276–281 (2010)

29. Lin, J., Wu, W.: A general rotation averaging method for granular materials. Granul. Matter **19**(3), 44 (2017)

30. Luna, B.Q., Remaitre, A., van Asch, T.W.J., Malet, J.P., van Westen, C.J.: Analysis of debris flow behavior with a one dimensional runout model incorporating entrainment. Eng. Geol. **128**, 63–75 (2012)

31. Mangeney, A., Roche, O., Hungr, O., Mangold, N., Faccanoni, G., Lucas, A.: Erosion and mobility in granular collapse over sloping beds. J. Geophys. Res. **115**(F03040) (2010). https://doi.org/10.1029/2009JF001462

32. McCoy, S.W., Kean, J.W., Coe, J.A., Staley, D.M., Wasklewicz, T.A., Tucker, G.E.: Evolution of a natural debris flow: in situ measurements of flow dynamics, video imagery, and terrestrial laser scanning. Geology **38**(8), 735–738 (2010)

33. McCoy, S.W., Kean, J.W., Coe, J.A., Tucker, G.E., Staley, D.M., Wasklewicz, T.A.: Sediment entrainment by debris flows: in situ measurements from the headwaters of a steep catchment. J. Geophys. Res. Earth Surf. **117**(F03016) (2012). https://doi.org/10.1029/2011JF002278

34. McCoy, S.W., Tucker, G.E., Kean, J.W., Coe, J.A.: Field measurement of basal forces generated by erosive debris flows. J. Geophys. Res. Earth Surf. **118**(2), 589–602 (2013). https://doi.org/10.1002/jgrf.20041

35. McDougall, S., Hungr, O.: A model for the analysis of rapid landslide motion across three-dimensional terrain. Can. Geotech. J. **41**(6), 1084–1097 (2004)

36. Medina, V.H., Bateman, A., Hurlimann, M.: A 2D finite volume model for bebris flow and its application to events occurred in the Eastern Pyrenees. Int. J. Sediment Res. **23**(4), 348–360 (2008)

37. Melosh, H.J.: Acoustic fluidization: can sound waves explain why dry rock debris appears to flow like a fluid in some energetic geologic events? Am. Sci. **71**(2), 158–165 (1983)

38. Montserrat, S., Tamburrino, A., Roche, O., Niño, Y., Ihle, C.F.: Enhanced run-out of dam-break granular flows caused by initial fluidization and initial material expansion. Granul. Matter **18**(1), 1–9 (2016)

39. Okada, Y., Ochiai, H.: Coupling pore-water pressure with distinct element method and steady state strengths in numerical triaxial compression tests under undrained conditions. Landslides **4**(4), 357–369 (2007)

40. Potyondy, D.O., Cundall, P.A.: A bonded-particle model for rock. Int. J. Rock Mech. Min. Sci. **41**(8), 1329–1364 (2004)

41. Reid, M.E., Iverson, R.M., Logan, M.A.T.T.H.E.W., LaHusen, R.G., Godt, J.W., Griswold, J.P.: Entrainment of bed sediment by debris flows: results from large-scale experiments. In: Genevois R., Hamilton, D.L., Prestininzi, A. (eds.) Proceedings of Fifth International Conference on Debris-flow Hazards Mitigation, Mechanics, Prediction and Assessment, Casa Editrice Universita La Sapienza, Rome, June 14–17, 2011, pp. 367–374 (2011)

42. Remaître, A., van Asch, ThWJ, Malet, J.P., Maquaire, O.: Influence of check dams on debris-flow run-out intensity. Nat. Hazards Earth Syst. Sci. **8**(6), 1403–1416 (2008)

43. Remaître, A., Malet, J.P, Maquaire, O.: Sediment budget and morphology of the 2003 Faucon debris flow (South French Alps): scouring and channel-shaping processes. In: Malet J.P., Remaitre A., and Bogaard T. (eds.) Proceedings of the International Conference on Landslide Processes: From géomorphologie Mapping to Dynamic Modelling, Strasbourg, France, February 6–7, 2009, pp. 75–80. CERG, Strasbourg (2009)

44. Salciarini, D., Tamagnini, C., Conversini, P.: Discrete element modeling of debris-avalanche impact on earthfill barriers. Phys. Chem. Earth **35**(3), 172–181 (2010)

45. Savage, S.B., Hutter, K.: The dynamics of avalanches of antigranulocytes materials from initiation to runout analysis. Acta Mech. **86**, 201–223 (1991)

46. Shodja, H.M., Nezami, E.G.: A micromechanical study of rolling and sliding contacts in assemblies of oval granules. Int. J. Numer. Anal. Methods Geomech. **27**(5), 403–424 (2003)

47. Skempton, A.W.: The pore-pressure coefficients A and B. Geotechnique **4**(4), 143–147 (1954)

48. Wu, F.C., Chou, Y.J.: Rolling and lifting probabilities for sediment entrainment. J. Hydraul. Eng. **129**(2), 110–119 (2003)

49. Xu, Q., Shang, Y.J., van Asch, ThWJ, Wang, S.T., Zhang, Z.Y., Dong, X.J.: Observations from the large, rapid Yigong rock slide-debris avalanche, southeast Tibet. Can. Geotech. J. **49**(5), 589–606 (2012)

50. Zhou, G.G., Ng, C.W.: Numerical investigation of reverse segregation in debris flows by DEM. Granul. Matter **12**(5), 507–516 (2010)